

## ORIGINAL ARTICLE

# Facets of diazotrophy in the oxygen minimum zone waters off Peru

Carolin R Loescher<sup>1</sup>, Tobias Großkopf<sup>2,3</sup>, Falguni D Desai<sup>2,4</sup>, Diana Gill<sup>2</sup>, Harald Schunck<sup>1,2</sup>, Peter L Croot<sup>5</sup>, Christian Schlosser<sup>6</sup>, Sven C Neulinger<sup>1</sup>, Nicole Pinnow<sup>1</sup>, Gaute Lavik<sup>7</sup>, Marcel MM Kuypers<sup>7</sup>, Julie LaRoche<sup>2,4</sup> and Ruth A Schmitz<sup>1</sup>

<sup>1</sup>Institute of General Microbiology, Christian Albrechts University Kiel, Kiel, Germany; <sup>2</sup>Helmholtz Center for Ocean Research Kiel (GEOMAR), Kiel, Germany; <sup>3</sup>School of Life Sciences, Gibbet Hill Campus, The University of Warwick, Coventry, UK; <sup>4</sup>Department of Biology, Dalhousie University, Halifax, Nova Scotia, Canada; <sup>5</sup>Earth and Ocean Sciences, School of Natural Sciences, National University of Ireland, Galway (NUI Galway), Ireland; <sup>6</sup>National Oceanography Centre Southampton, University of Southampton, Waterfront Campus, Southampton, UK and <sup>7</sup>Max-Planck-Institute for Marine Microbiology, Bremen, Germany

**Nitrogen fixation, the biological reduction of dinitrogen gas (N<sub>2</sub>) to ammonium (NH<sub>4</sub><sup>+</sup>), is quantitatively the most important external source of new nitrogen (N) to the open ocean. Classically, the ecological niche of oceanic N<sub>2</sub> fixers (diazotrophs) is ascribed to tropical oligotrophic surface waters, often depleted in fixed N, with a diazotrophic community dominated by cyanobacteria. Although this applies for large areas of the ocean, biogeochemical models and phylogenetic studies suggest that the oceanic diazotrophic niche may be much broader than previously considered, resulting in major implications for the global N-budget. Here, we report on the composition, distribution and abundance of *nifH*, the functional gene marker for N<sub>2</sub> fixation. Our results show the presence of eight clades of diazotrophs in the oxygen minimum zone (OMZ) off Peru. Although proteobacterial clades dominated overall, two clusters affiliated to spirochaeta and archaea were identified. N<sub>2</sub> fixation was detected within OMZ waters and was stimulated by the addition of organic carbon sources supporting the view that non-phototrophic diazotrophs were actively fixing dinitrogen. The observed co-occurrence of key functional genes for N<sub>2</sub> fixation, nitrification, anammox and denitrification suggests that a close spatial coupling of N-input and N-loss processes exists in the OMZ off Peru. The wide distribution of diazotrophs throughout the water column adds to the emerging view that the habitat of marine diazotrophs can be extended to low oxygen/high nitrate areas. Furthermore, our statistical analysis suggests that NO<sub>2</sub> and PO<sub>4</sub><sup>3-</sup> are the major factors affecting diazotrophic distribution throughout the OMZ. In view of the predicted increase in ocean deoxygenation resulting from global warming, our findings indicate that the importance of OMZs as niches for N<sub>2</sub> fixation may increase in the future.**

*The ISME Journal* (2014) 8, 2180–2192; doi:10.1038/ismej.2014.71; published online 9 May 2014

**Subject Category:** Microbial ecology and functional diversity of natural habitats

**Keywords:** heterotrophic N<sub>2</sub> fixation; *nifH* diversity; oxygen minimum zone off Peru

## Introduction

High primary productivity in upwelling systems associated with eastern boundary currents results in enhanced oxygen (O<sub>2</sub>) consumption at depth related to the degradation of sinking organic matter (Duce *et al.*, 2008).

The reduced O<sub>2</sub> concentrations in subsurface waters favours N-loss processes, P release (Ingall and Jahnke, 1994; Deutsch *et al.*, 2007) and may

increase iron bioavailability, conditions that overall are favourable for N<sub>2</sub> fixation (Deutsch *et al.*, 2001; Deutsch *et al.*, 2007). Similar to N<sub>2</sub> fixation, other N-cycle processes such as anaerobic ammonium oxidation (anammox), denitrification and nitrification are sensitive to O<sub>2</sub>, thus low O<sub>2</sub> concentrations make oxygen minimum zones (OMZs) hotspots for N-turnover processes (Capone, 2008; Codispoti, 2010; Kalvelage *et al.*, 2013). Further, field observations have demonstrated that N<sub>2</sub> fixation occurs concurrently with fixed N-loss processes (Halm *et al.*, 2009; Fernandez *et al.*, 2011; Gandhi *et al.*, 2011), suggesting that OMZs, such as the large and persistent OMZ present in the eastern tropical Pacific Ocean off Peru, are an ideal environment for marine diazotrophy (Bopp *et al.*, 2002).

Correspondence: CR Loescher, Institute of Microbiology, Christian Albrechts University Kiel, Am Botanischen Garten 1-9, Kiel 24118, Germany.

E-mail: cloescher@ifam.uni-kiel.de

Received 9 August 2013; revised 20 March 2014; accepted 30 March 2014; published online 9 May 2014

$N_2$  fixation rates in the ocean have largely been underestimated owing to a methodological bias (Grosskopf *et al.*, 2012). Particularly, the contribution to fixed N budget from diazotrophs other than the classically known cyanobacteria, for example, the filamentous diazotroph *Trichodesmium*, may have been disproportionately underestimated owing to an uneven distribution of label in the classical  $^{15}N_2$  incubation experiments, which results in lower labeling efficiency of non-buoyant organisms (Grosskopf *et al.*, 2012). This realization, together with the growing number of studies on the phylogenetic diversity of diazotrophs (Farnelid *et al.*, 2011; Fernandez *et al.*, 2011; Turk *et al.*, 2011), demonstrates the need to investigate the diazotrophic community in environments that were previously not considered important for  $N_2$  fixation. Reports on the diversity of the *nifH* gene in OMZ waters suggested that the detected diazotrophic communities differ strongly from those present in oligotrophic oceanic waters (Zehr and Turner, 2001; Falcon *et al.*, 2002; Langlois *et al.*, 2005; Fernandez *et al.*, 2011; Hamersley *et al.*, 2011; Jayakumar *et al.*, 2012; Farnelid *et al.*, 2013). Along the Californian coast, the OMZ off Peru and Chile, in the Arabian Sea and in two basins of the Baltic Sea, diverse *nifH* gene sequences mostly related to heterotrophic proteobacteria have previously been identified (Fernandez *et al.*, 2011; Hamersley *et al.*, 2011; Jayakumar *et al.*, 2012; Farnelid *et al.*, 2013). The role and importance of those non-cyanobacterial diazotrophs for the oceanic fixed N budget is currently unclear due to the limited information on their biogeographical distribution, abundance and activity. To shed light on diazotrophy in OMZs and the potential role of non-phototrophic  $N_2$  fixers, we conducted a large-scale survey of functional gene abundances,  $O_2$  and nutrients, such as nitrite ( $NO_2^-$ ), nitrate ( $NO_3^-$ ), ammonia ( $NH_4^+$ ), phosphate ( $PO_4^{3-}$ ), iron (Fe) concentrations and  $N_2$  fixation rates complemented with glucose enrichment and oxygen manipulation experiments throughout the OMZ off Peru in the eastern tropical South Pacific (ETSP).

## Materials and methods

### Hydrographic parameters and nutrients

Samples for salinity,  $O_2$  and macro-nutrient analysis ( $NO_3^-$ ,  $NO_2^-$ ,  $NH_4^+$  and  $PO_4^{3-}$ ) were collected from a 24 Niskin bottle rosette equipped with a CTD (Conductivity, Temperature, Depth) sensor or from a pump-CTD. The pump-CTD used during M77/3 is a CTD, equipped with a pump that transfers water from depth directly up into the lab. CTD,  $O_2$ , fluorescence, turbidity, and acoustic doppler counter profiler measurements can be combined with continuous water sampling over a water column of 350 m depth in high resolution (1 m maximum) along vertical profiles.

$O_2$  concentrations were determined according to the Winkler method; salinity and nutrient

concentrations were determined as previously described (Grasshoff *et al.*, 1999).  $P^*$  was calculated from phosphate and nitrate measurements according to Deutsch *et al.* (2007):  $P^* = PO_4^{3-} - NO_3^- / r_{16:1}$ , where  $r_{16:1}$  is the ratio of nitrate to phosphate at Redfield conditions (Deutsch *et al.*, 2007).

### Trace metal sampling and analysis

Seawater samples were obtained using the modified Teflon-coated PVC General Oceanics (Miami, FL, USA) GoFlo (8 l) bottles on a trace metal clean hydrowire using established protocols (Bruland *et al.*, 1979). After recovery, the bottles were transferred into a class 100 clean lab container and filtered immediately through a 0.2- $\mu$ m membrane filter (Sartorius, Göttingen, Germany) under slight nitrogen overpressure (0.2–0.3 bar) into 1 liter acid-washed low-density polyethylene bottles. The seawater samples for trace metal analysis were acidified in a laminar flow hood with quartz-distilled concentrated hydrochloric acid (6 M QD-HCl) to pH 1.8 ( $17.8 \mu\text{mol H}^+ \text{l}^{-1}$ ) and stored in the dark until analysis half a year later.

Dissolved Fe concentrations were determined via graphite furnace-atom absorption spectrometry (GF-AAS) (Zeemann Atomic Absorption Spectrometer 4100ZL, Perkin Elmer, Waltham, MA, USA). The samples were analysed by a method previously outlined by Danielson *et al.* (1978) and Bruland *et al.* (1979) and described in detail by Grasshoff *et al.* (1999). The accuracy of the analytical procedure was evaluated by measurement of the certified seawater standard NASS-5 (National Research Council of Canada) and the SAFe inter-comparison standard. Our values for NASS 5 agreed within the stated values for NASS 5 and our SAFe data (SAFe S:  $0.109 \pm 0.013 \text{ nmol kg}^{-1}$  Fe; SAFe D2:  $0.81 \pm 0.13 \text{ nmol kg}^{-1}$  Fe) were close to the average consensus values for Fe (NASS 5:  $3.70 \pm 0.63 \text{ nmol kg}^{-1}$ ; SAFe S:  $0.093 \pm 0.008 \text{ nmol kg}^{-1}$ ; SAFe D2:  $0.933 \pm 0.023 \text{ nmol kg}^{-1}$ ). The precision for replicate analyses was between 3% at the concentrations found in this study. The analytical Fe blank was determined by re-extraction of samples and was found to be  $0.041 \pm 0.024 \text{ nmol kg}^{-1}$  ( $3\sigma$  detection limit =  $0.079 \text{ nmol kg}^{-1}$ ).

### Molecular genetic methods

Samples for the extraction of DNA/RNA were taken by filtering a volume of about 2 l (exact volumes and filtration times were determined and recorded for each sample) of seawater through 0.2- $\mu$ m polyether-sulfone membrane filters (Millipore, Billerica, MA, USA). The filters were immediately frozen and stored at  $-80^\circ\text{C}$ .

DNA and RNA were extracted using the Qiagen DNA/RNA All prep Kit (Qiagen, Hilden, Germany) according to the manufacturer's protocol. DNA concentrations were determined fluorometrically

using the PicoGreen (Invitrogen, Carlsbad, CA, USA) as described in the manufacturer's protocol using a Fluorometer (Fluorocan Ascent Labsystems, Helsinki, Finland). A standard dilution series (2.5–100 pg  $\mu\text{l}^{-1}$ ) was used for absolute quantification. Residual DNA was removed from the purified RNA by a DNase I treatment (Invitrogen). The RNA was checked for potential DNA contamination by 16S rDNA PCR amplification using the universal primer set 27F and 1492R (Lane *et al.*, 1991) before reverse transcription and by a nested *nifH* PCR as described above. RNA concentrations were determined similar to DNA concentrations using the fluorescent dye RiboGreen (Invitrogen) and a RNA standard dilution series (2.5–80 pg  $\mu\text{l}^{-1}$ ).

The extracted RNA was reverse transcribed to cDNA using the Superscript III First Strand synthesis Kit (Invitrogen) following the manufacturer's protocol with primers *nifH2* and *nifH3* (Zani *et al.*, 2000; Langlois *et al.*, 2005).

*NifH* was amplified by a nested PCR with primers according to Zani *et al.* (2000) and Langlois *et al.* (2005), using 0.1  $\mu\text{l}$  GoTaq polymerase (Promega, Madison, WI, USA) in a final volume of 25  $\mu\text{l}$ . Based on *nifH* sequence information of clusters P1–P8, quantitative PCR (qPCR) primers and TaqMan MGB probes (6-carboxyfluorescein reporter) were designed with the Primer Express software package (Life Technologies, Darmstadt, Germany); oligonucleotide sequences and qPCR conditions are given in Table 1.

Primers and probes were checked against the NCBI database and an ARB *nifH* database using BLAST search to ensure that they were specific for the selected *nifH* cluster. Standards for the different *nifH* clusters were obtained by cloning the *nifH* amplicons using the Topo TA Cloning Kit (Invitrogen). Plasmid extraction and purification was performed using the Qiagen plasmid purification kit according to the manufacturer's protocol; plasmid concentrations were determined using a NanoDrop ND-1000 spectrophotometer (PeqLab, Erlangen, Germany) and diluted to 4 pg  $\mu\text{l}^{-1}$ , which corresponds to  $10^7$  target sequence copies in a 5- $\mu\text{l}$  volume. Serially diluted plasmid standards were used to calculate copy numbers in the qPCR assays. The primer and probe set we used to quantify UCYN-B in this study has been previously described (Langlois *et al.*, 2008).

The specificity of the qPCR primer and probe sets was confirmed by testing for cross-reactivity and sensitivity against each available standard in our lab, diluted to  $10^4$  and  $10^5$  *nifH* copies. DNA amplification signals were detected only for the homologous phylotype. Additionally, the sensitivity of the primers and probes in a mixed DNA sample was tested in combinations of serially diluted standards mixed in ratios ranging from  $10^7:10^1$  to  $10^1:10^7$  copies of the specific and unspecific standard, which did not result in significant changes in the linear regressions, indicating that the presence of various amounts of closely related DNA sequences does not affect the quantification of a specific phylotype. qPCR mixtures contained 1  $\times$  TaqMan PCR buffer (Life Technologies), 100 nM TaqMan probe, 5 pmol  $\mu\text{l}^{-1}$  each of the forward and reverse primers, 400 ng  $\mu\text{l}^{-1}$  bovine serum albumin, 3  $\mu\text{l}$  PCR water, and 5  $\mu\text{l}$  of either standard or environmental sample. Addition of bovine serum albumin to the reactions was performed to avoid PCR inhibition without affecting standard curves or detection limits as previously described in Langlois *et al.* (2008). Environmental DNA samples and standards were run in duplicates. To avoid degradation, extracted DNA was frozen in aliquots and thawed only once for qPCR determination. Non-template controls were run in duplicate for each primer and probe set and were undetectable after 45 cycles, which translates into a theoretical detection limit of the qPCR assays of one *nifH* gene copy. The analytical detection limit depends on several other factors, for example, the amount of seawater filtered, the elution volume after extraction and the amount of sample loaded setting the detection limit for our samples to 60 copies  $\text{l}^{-1}$ . Accordingly, we considered samples with  $C_T$  values  $<36$  ( $<10^2$  copies  $\text{l}^{-1}$ ) detectable but not quantifiable, similar to previous studies (Langlois *et al.*, 2008).

*AmoA* PCRs and qPCRs were performed as described in Loescher *et al.* (2012); *nirS* and *hzo* were amplified according to Lam *et al.* (2007) and Schmid *et al.* (2008), respectively.

Cloning of PCR amplicons was performed using the Topo TA Cloning Kit (Invitrogen) according to the manufacturer's instructions. Sanger sequencing was carried out by the Institute of Clinical Molecular

**Table 1** Oligonucleotide sequences and quantitative PCR conditions

Cluster	Reference sequence	Forward primer 5'–3'	Reverse primer 5'–3'	Probe	Annealing temperature (°C)
P1	M773_3_70_4	GGACTACATTCGGACTAG	GTCGTAACCACGATCTAG	TCTTCAAATCCGGCGTCCCG (antisense)	60
P2	M773_3_150_7	GGTGTCTATGTGTTGAA	GTAGAGTTACGAATTGG	TGCCTAGCACATCATAGATCAC (antisense)	50
P3	M773_56_100_1	CACAGTTAGAGAGGTAGG	CAAGGTCGTCAGTAAAAG	AGCTCGACAAGGTAATGTTTACA (sense)	54
P4	M773_22_30_1	CTCGCACAGAAATCAGTG	GCATGTTAATGGAAGTGATG	ACGTGCAACTCGAAGACATCCG (sense)	60
P5	M773_56_100_11	GGAAGTCTTACTTGAAGG	CACCATTTTCTCAAGAA	ATTGCTGTAATAACGCCCTCTGC (antisense)	60
P6	M773_56_85_3	GCTCAATCTACAATTATGC	GCTGTAATAACTCCTCTAC	ACCACCTGACTCAGTACAATTAATGT (antisense)	50
P7	M773_28_115_1	GGTCTGTGTAAGACATC	CGAAGTCTAAGTCTTCTTC	ATCGCTGTGATTACACCACGAC (antisense)	52
P8	M774_800_m_11B14a	ACTCGTCTGATCTTTCAC	TTAATACATCTTCCAGTTCCA	AAAGCACAGAACACCATCATG (antisense)	52



Biology, Kiel, Germany. Nucleotide sequences were analysed using the ClustalW multiple alignment tool on a 321-bp fragment for *nifH*. Sequences were submitted to Genbank and were analysed using the ClustalW multiple alignment tool on a 321-bp fragment for *nifH*, sequence differences were set on a minimum of 5% and phylogenetic trees were made using the distance-based neighbor-joining analysis.

#### Statistical analysis

The impact of environmental parameters on the abundance and distribution of *nifH* clusters (copies l<sup>-1</sup>) as determined by qPCR was explored by redundancy analysis (RDA) based on 316 cases. Computations were performed in R v3.0.2 (R\_Core\_Team, 2013) by using the R package vegan (Oksanen *et al.*, 2013). *nifH* cluster counts were subjected to Hellinger transformation in order to make them compatible with RDA (Legendre and Gallagher, 2001; Stratil *et al.*, 2013).

The most parsimonious RDA model was determined via stepwise selection with vegan's function *ordistep* considering depth as well as concentrations of O<sub>2</sub>, NO<sub>2</sub><sup>-</sup>, NO<sub>3</sub><sup>-</sup> and PO<sub>4</sub><sup>3-</sup> as explanatory variables. Variable depth substitutes temperature and salinity to avoid collinearity and was used as a surrogate for variables changing with depth (for example, trace metals or viral infection pressure). Wherever possible, O<sub>2</sub> concentrations determined according to the Winkler method were used. A correlation test between Winkler and CTD oxygen data showed that the two variables were strongly correlated ( $R(166) = 0.98$ ,  $R^2 = 0.96$ ,  $P < 0.001$ ). Correspondingly, a Wilcoxon signed rank test on existing data pairs did not indicate any systematic differences between Winkler and CTD oxygen data (two-sided test,  $n = 168$ ,  $P = 0.41$ ). Missing Winkler measurements were thus substituted by data from the CTD oxygen sensor. Significance of the selected model and of marginal effects (that is, of each parameter in the presence of all other parameters) was determined in permutation tests with 1000 random permutations.

#### <sup>15</sup>N<sub>2</sub> seawater incubations

Seawater incubations were performed in triplicate at six stations in the OMZ off Peru (M77/3) according to an existing protocol (Montoya *et al.*, 1996). In detail, seawater from the OMZ was sampled from a pump-CTD system and directly filled into 2 l glass bottles (Schott-Duran, Wertheim, Germany) from the bottom, allowing the displacement of about one bottle volume through the opening before closing the bottle bubble free with a Teflon covered butyl septum cap. Samples from the surface were taken by either the pump-CTD system or the conventional CTD and filled in 4.5 l polycarbonate bottles (Nalgene, Rochester, NY, USA) with Teflon-coated butyl rubber septum caps. Bottles were spiked with 2 ml (2-l flasks) or 4.5 ml (4.5-l

flasks) of 98% <sup>15</sup>N<sub>2</sub> gas (Sigma-Aldrich, St Louis, MO, USA). This method has recently been found to underestimate the true N<sub>2</sub> fixation rates (Mohr *et al.*, 2010), therefore the rates measured in this study can be taken as minimum values.

For carbon fixation measurements, NaH<sup>13</sup>CO<sub>3</sub> (Sigma-Aldrich) was dissolved in sterile deionized water (>18.2 MOhm cm<sup>-1</sup>, MilliQ, Millipore) (1 g/50 ml) and 0.5 ml (2-l bottles) or 1 ml (4.5-ml bottles) were added to the incubations with a syringe (~3.5 atom % final). For glucose and oxygen addition experiments, 500 ml of seawater from the same location was aerated by vigorously bubbling with sterile filtered air from a compressor for 15 min. The amount of seawater leading to a final concentration of 10 μmol l<sup>-1</sup> dissolved oxygen (depending on temperature conditions, for example, 39 ml l<sup>-1</sup> at 12 °C) was added with a syringe to the bottom of the incubation bottles, while water from the top was replaced. Glucose (Sigma-Aldrich) was dissolved in MilliQ water (1.44 g l<sup>-1</sup>), and the concentrated solution was added through the septum with a syringe to yield a final concentration of 2 μM glucose. After amendments, bottles were inverted 100 times. Bottles from surface water were stored on deck in a seawater-cooled Plexiglas incubator covered with blue light foil (blue-lagoon, Lee filters, Andover, UK) that mimics the light environment of a 10-m depth. Samples from the OMZ were stored at 12 °C in the dark. After 24 h of incubation, 0.7–2.5 l of seawater were filtered onto precombusted (450 °C, 5 h) 47-mm diameter GF/F filters (Whatman, Maidstone, UK) under gentle vacuum (–200 mbar). The filtrations were stopped after 1 h, as high particle load of surface water often led to a clogging of the filters. Filters were oven dried (50 °C) for 24 h and stored over desiccant until analysis. Environmental samples of 2 l untreated seawater were filtered and prepared in the same way to serve as blank values. For isotope analysis, GF/F filters were acidified over fuming HCl overnight in a desiccator. Filters were then oven-dried for 2 h at 50 °C and pelletized in tin cups. Samples were analysed for particulate organic carbon and particulate organic nitrogen (PON) and isotopic composition using a CHN analyzer (Carlo Erba EA 1108, Milano, Italy) coupled to an isotope ratio monitoring mass spectrometer (Thermo Finnigan Delta S, Waltham, MA, USA). The content of PON of most samples exceeded 10 μg l<sup>-1</sup>. Lowest PON values were measured on the deep water offshore stations (~3 μg l<sup>-1</sup>). Details of the statistical evaluation of the glucose and oxygen addition experiments are given in the Supplementary Information.

## Results and discussion

### *Diversity and distribution of atypical nifH clusters in the OMZ off Peru*

We conducted two consecutive expeditions with R/V *Meteor* in January (M77/3) and February 2009 (M77/4)

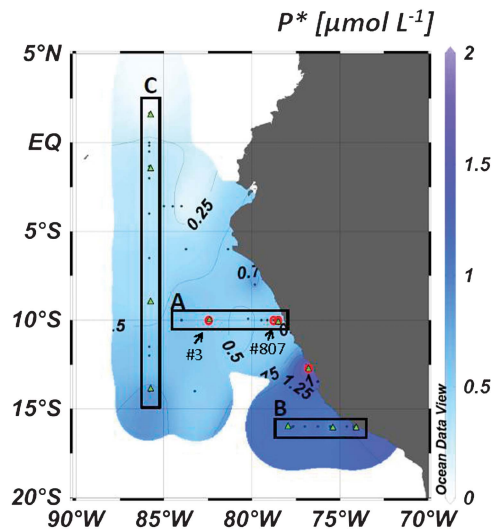


**Figure 1** Surface distribution of  $P^*$  ( $\mu\text{mol l}^{-1}$ ) in the Peruvian OMZ, three transects (A, B and C) are marked with black boxes; red circles indicate the stations of  $\text{N}_2$  fixation experiments, green triangles indicate the stations, which were selected for clone library construction.

to the OMZ off Peru. Samples from vertical depth profiles were collected along two transects from the shelf to the open ocean throughout the OMZ (Figure 1, transects A and B, M77/3) and a north–south transect in offshore waters (Figure 1, transect C, M77/4). On the shelf, the water column was anoxic between 20 m and 80 m (Supplementary Figure S1), while the oxycline deepened offshore reaching anoxic conditions at  $\sim 100$  m. Excess phosphorous ( $P^*$ ; representing the excess of P relative to the standard N quota) previously implicated in the control of  $\text{N}_2$  fixation (Deutsch *et al.*, 2007) was pervasive in the OMZ as well as in the surface layer (Figure 1, Supplementary Figure S1), with highest excess concentrations (up to  $2 \mu\text{M}$ ) on the shelf.

A total of  $\sim 600$  *nifH* sequences were obtained from clone libraries (384 from DNA and 249 from cDNA libraries) constructed from 29 samples collected at 12 stations along transects A, B and C. Samples were chosen according to the detected  $\text{O}_2$  saturation to cover a spectrum reaching from full  $\text{O}_2$  saturation in surface waters, hypoxic saturations ( $15\text{--}75 \mu\text{mol l}^{-1}$ ) to the OMZ core ( $[\text{O}_2] < 15 \mu\text{mol l}^{-1}$ ) (Supplementary Figure S1).

The *nifH* sequences grouped into nine clusters (further referred to as P1–P8 and UCYN-B; Figure 2). Those clusters were in large part (73%) recovered from OMZ waters ( $[\text{O}_2] \leq 15 \mu\text{mol l}^{-1}$  at  $\sim 10$ -m depths onshore and at  $\sim 50\text{--}100$ -m depths offshore (Kalvelage *et al.*, 2013), see Supplementary Figure S1) in samples collected below the euphotic zone (Chl a was below the detection limit at  $\sim 50$ -m depth onshore at  $10^\circ\text{S}$  and at  $\sim 120$ -m depth offshore (Franz *et al.*, 2012)). This indicates that the diazotroph community was most likely non-photoautotrophic. Combined with the phylogenetic analysis of *nifH* genes, this adds to

the growing awareness of the importance of non-cyanobacterial diazotrophs for  $\text{N}_2$  fixation in the ocean (Fernandez *et al.*, 2011; Hamersley *et al.*, 2011; Jayakumar *et al.*, 2012; Farnelid *et al.*, 2013). The presence of those clusters points towards a potential to fix  $\text{N}_2$  in the OMZ off Peru.

P1 and P2 *nifH* clades have never been reported before and were the most distant clades in our study compared with previously detected marine *nifH* genes. In addition to those two novel deep branching clusters, clusters P3–P7 were phylogenetically related to proteobacterial *nifH* genes amplified from hypoxic basins in the Californian Bight and the OMZ off Peru and Chile (97–99% similarity; see Supplementary Table S1 for sequence overlaps with previous studies). Sequences related to P4 and P8 clusters were previously detected in the tropical South Pacific Ocean (Fernandez *et al.*, 2011; Halm *et al.*, 2012) (Supplementary Table S1). The P4 sequences were mainly present in clone libraries derived from shelf waters (Figure 1, M77/3 transects A and B) while P8 sequences were recovered from clone libraries prepared from samples collected along a north–south transect at  $85.83^\circ\text{W}$  in open ocean waters during M77/4 (Figure 1, transect C from surface waters down to 350 m). Sequences from clusters P3, P7 and P8 have been detected before in the Indian Ocean (Farnelid *et al.*, 2011).

Cluster-specific qPCR-TaqMan assays targeting the *nifH* genes of the novel diazotrophs revealed that clusters P1 and P4 were dominating the diazotrophic community from the shelf to about  $83^\circ\text{W}$  at  $10^\circ\text{S}$  and to  $77^\circ\text{W}$  at  $16^\circ\text{S}$  ( $< 10^5$  *nifH* copies  $\text{l}^{-1}$ , Figure 3), accounting for up to 93% of total *nifH* onshore at  $10^\circ\text{S}$  (from surface down to 100 m). The P1 cluster was generally associated with deeper waters (100–300 m) with low or non-detectable  $\text{O}_2$  concentrations and high  $\text{PO}_4^{3-}$  (P1 abundances  $> 10^3$  copies  $\text{l}^{-1}$  were present at  $\text{O}_2 < 5 \mu\text{M}$  and  $\text{PO}_4^{3-} > 2.4 \mu\text{mol kg}^{-1}$ ) concentrations, while other clusters (P2, P3, P4,) were present in surface to subsurface waters (Figure 3 and Supplementary Figure S1). Cluster P8 was present throughout the Peruvian OMZ (Figure 3, Supplementary Figure S2) dominating the nutrient-depleted open ocean region along the north–south offshore transect quantitatively (transect C, Figure 1, Supplementary Figure S2), with abundances reaching up to  $10^6$  *nifH* copies  $\text{l}^{-1}$ . *nifH* gene sequences belonging to the filamentous non-heterocystous cyanobacterium *Trichodesmium* sp., the diatom endosymbiont *Richelia* sp. or *Candidatus* Atelocyanobacterium thalassa, which are all considered key diazotrophs in oligotrophic surface waters of the ocean (Church *et al.*, 2005), were not recovered from our clone libraries; however, our sequencing approach allows only the detection of the predominant clusters. *Crocospaera*-like *nifH* (Zehr *et al.*, 1998) was the only cyanobacterial sequence recovered from some of our clone libraries (1 out of  $\sim 384$  sequences, 95.7% sequence identity to *C. watsonii* WH8501, GeneBank no.: AF300829)).

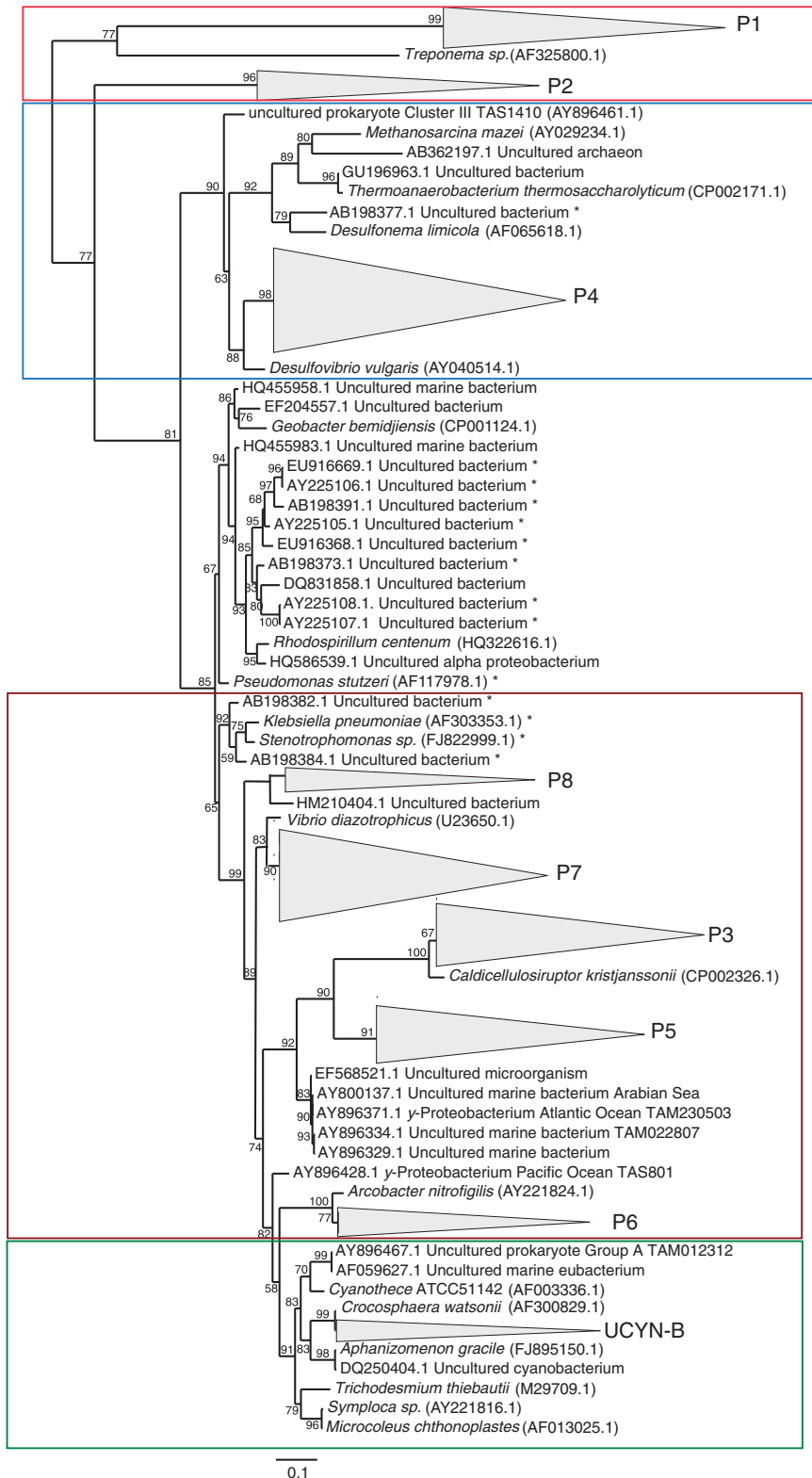


**Figure 2** Phylogenetic tree based on the analysis of ~600 *nifH* gene and transcript nucleotide sequences retrieved in this study. The detected clusters are indicated with grey triangles. Cyanobacterial sequences are highlighted in green, proteobacterial sequences are highlighted in brown, Cluster III sequences as defined by Zehr et al. (2003) are shown in blue and two distant clusters are highlighted red. Bootstrapped values (%) > 50, out of 100 are shown on branches. The scale bar represents 10% estimated sequence divergence. Sequences marked with an asterisk indicate likely contaminated PCR products previously reported by Turk et al. (2011), the detected clusters are mostly distant from those sequences.



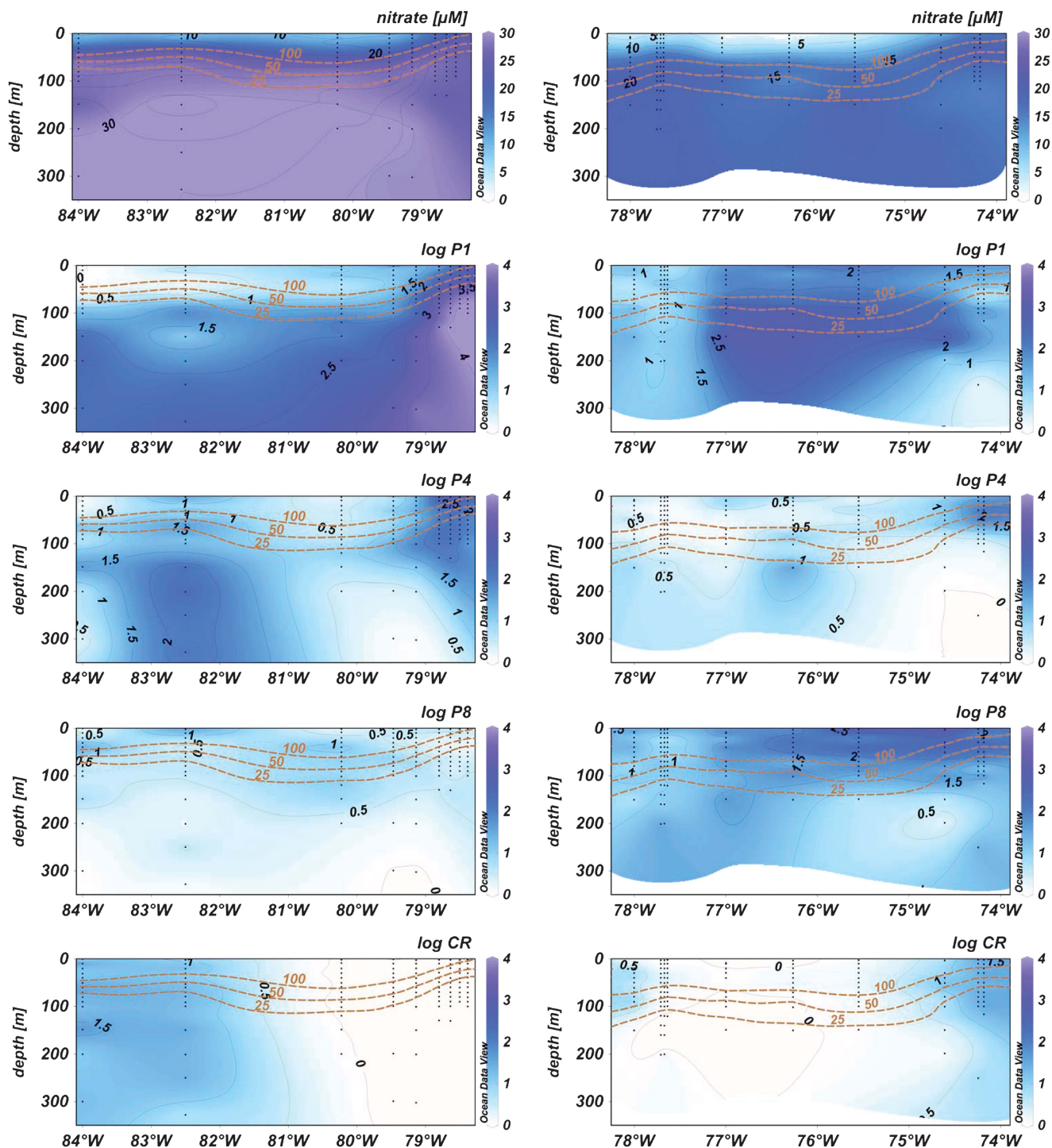


**Figure 3** Distribution of  $\text{NO}_3^-$  and the detected *nifH* clusters:  $\text{NO}_3^-$  ( $\mu\text{M}$ ), *nifH* clusters P1, P4, P8 and *Crocospheara* ( $\log_{10}$  copies  $\text{l}^{-1}$ ), the oxycline ( $\mu\text{M O}_2$ ) is indicated with brown contour lines along (left)  $10^\circ\text{S}$  and (right)  $16^\circ\text{S}$  as marked A and B on the map (Figure 1).

The UCYN-B-like cluster was mainly present in abundances close to the detection limit offshore in waters with high  $\text{NO}_3^-$  concentrations, at  $16^\circ\text{S}$ . *nifH* genes affiliated to UCYN-B were detected on the shelf as well ( $1.8 \times 10^2$  copies  $\text{l}^{-1}$ , Figure 3); however, it is unclear whether UCYN-B like diazotrophs had an active role in fixing  $\text{N}_2$  in the OMZ off Peru during our study.

A RDA indicated that a model containing depth,  $\text{NO}_2^-$  and  $\text{PO}_4^{3-}$  could explain roughly one-tenth of the total variance in the transformed *nifH* count data (Figure 4).

The dominant clusters P1, P4, P8 and, to a lesser extent, UCYN-B showed the most pronounced response to environmental variables in the parsimonious model (Figure 4, Supplementary Figure S3).

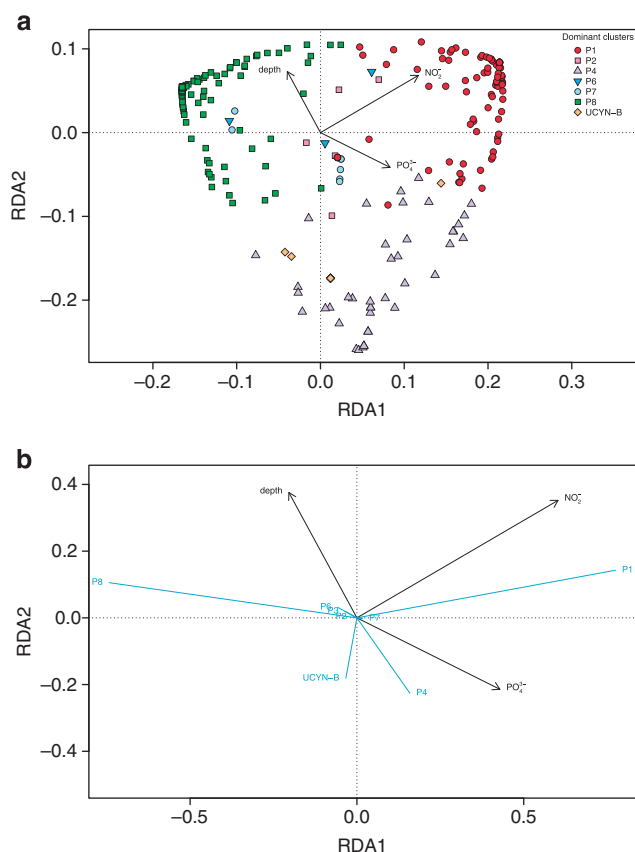


**Figure 4** Redundancy analysis (RDA) of Hellinger-transformed *nifH* cluster abundances. **(a)** The distance biplot (scaling 1) shows relations between samples (weighted sums of species scores) and environmental variables in the parsimonious model. **(b)** Correlation biplot (scaling 2) shows relations between *nifH* cluster vectors and environmental variables in the parsimonious model.

Cluster P1 and P8 occupied complementary habitats, being positively and negatively correlated with NO<sub>2</sub><sup>-</sup> and PO<sub>4</sub><sup>3-</sup> concentrations, respectively. Although P1 dominates the shelf OMZ, P8 is almost exclusively present offshore (transect C, Figure 1); this distribution may be explained by several factors, such as nutrient and/or trace metal quotas, or different requirements for organic material. P8 is identical with a cluster previously identified in the South Pacific Gyre (Gamma 4; Halm *et al.*, 2012), suggesting that those organisms prefer more oligotrophic conditions. Cluster P4 was negatively correlated with depth and positively with PO<sub>4</sub><sup>3-</sup>, thus P4 occupies a very limited habitat in the OMZ, associated with the upper OMZ, where O<sub>2</sub> is still available at low concentration while sinking particles potentially provide chemical energy to fuel their metabolism.

O<sub>2</sub> and NO<sub>3</sub><sup>-</sup> had no effect on the relation between *nifH* clusters and the other environmental variables (Supplementary Figure S4) and were dropped from the parsimonious model during the analyses. From the analysis of variance inflation factors, it became clear that the oxygen effect might be substituted by the effect of phosphate. The lack of an effect from

NO<sub>3</sub><sup>-</sup> might be explained by the findings of Grosskopf and LaRoche (2012) that assimilatory nitrate uptake loses its energetic advantage over N<sub>2</sub> fixation in low O<sub>2</sub> environments. Moreover, in our model, depth might substitute physical variables, such as temperature and salinity, as all of them mark different water masses collinearly. Thus, the observed depth-dependent *nifH* distribution patterns can potentially be linked to the presence of different water masses. Depth can further be thought of as a surrogate for secondary biotic and abiotic environmental variables. For example, the concentration of the trace metals such as Ni, Cu and Zn increase linearly with depth in our study area (Christian Schlosser, unpublished). The reason we did not incorporate trace metals into our statistical model is that we would have had to waive too many data points due to sparse sampling. It will be advantageous in future studies to directly measure these and other variables in addition to those we identified as relevant.

#### *In situ* N<sub>2</sub> fixation

Measurements of the incorporation of <sup>15</sup>N<sub>2</sub> into particulate organic material (PON) revealed low but detectable N<sub>2</sub> fixation rates throughout the OMZ, potentially favoured by P\* (Figure 1, Supplementary Figure S1). In addition, dissolved iron was present in high concentrations in the waters on the shelf (10–60 nmol kg<sup>-1</sup> in the OMZ core) and decreased towards open ocean locations down to 0.2–1.9 nmol kg<sup>-1</sup> in the core of the OMZ in line with observations from earlier studies (Hong and Kester, 1986; Hutchins *et al.*, 2002; Bruland *et al.*, 2005). A broad maximum of N<sub>2</sub> fixation extending into the OMZ (beginning at ~40 m) could be observed at 10°S from 79.134°W to 81.361°W with up to 0.4 nmol N l<sup>-1</sup> d<sup>-1</sup> at 200 m depth close to the coast, slightly decreasing towards offshore (Supplementary Figures S5 and S6). Further south on the Peruvian shelf (no.19, 12°21.88'S, 77°0.00'W), water column N<sub>2</sub> fixation rates increased, showing higher activity in surface waters than at depth, consistent with low N:P ratios (resulting in high P\*, Supplementary Figure S1) and high dissolved iron concentrations (up to 267 nmol kg<sup>-1</sup>, Figure 5), there. Highest N<sub>2</sub> fixation rates of 24.8 ± 8.4 nmol N l<sup>-1</sup> d<sup>-1</sup> were measured in surface waters and at lower rates in deeper waters, where *nifH* of UCYN-B, P1 and P7 was expressed (Figure 5). At this station, the water column below the mixed layer (~20 m) was completely anoxic and hydrogen sulfide (H<sub>2</sub>S) was present from bottom to 26 m depth (Figure 5 (Schunck *et al.*, 2013)). Below 30-m depth, the water was depleted in NO<sub>3</sub><sup>-</sup> and NO<sub>2</sub><sup>-</sup>, the key substrates for anammox and denitrification, suggesting a limitation of N-loss activity by substrate unavailability; however, both processes were active at that station (Kalvelage *et al.*, 2013). Ammonia was present in concentrations of 2–4 μM



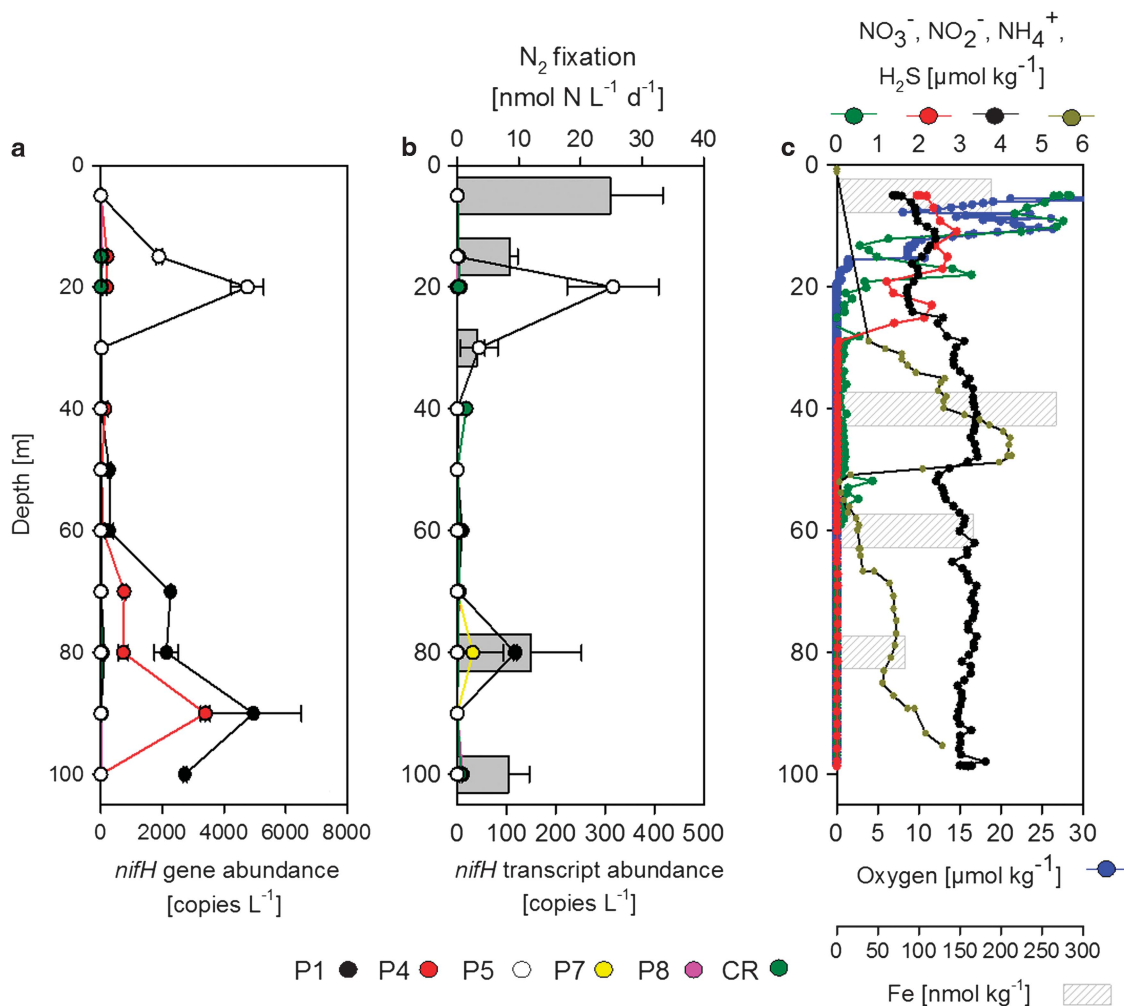


**Figure 5** Vertical distribution of (a) the *nifH* gene abundance, (b) the measured N<sub>2</sub> fixation and *nifH* gene expression (samples were specifically collected for RNA extraction), and (c) chemical parameters (O<sub>2</sub>, NO<sub>3</sub><sup>-</sup>, NO<sub>2</sub><sup>-</sup>, NH<sub>4</sub><sup>+</sup>, H<sub>2</sub>S, Fe) at a coastal sulphidic station (M77/3, no.19, 12°21.88'S, 77°0.00'W).

below the oxycline, which is classically assumed to inhibit N<sub>2</sub> fixation (Ullrich *et al.*, 1990), but integrated water column N<sub>2</sub> fixation exceeded 800 μmol N m<sup>-2</sup> d<sup>-1</sup>, a rate comparable to those reported from major *Trichodesmium* blooms (Capone *et al.*, 2005). The peak in P1 *nifH* expression present at 80 m along with a maximum in N<sub>2</sub> fixation here indicates an involvement of this cluster in N<sub>2</sub> fixation at depth. However, P1 sequences are the closest related to cluster IV (Zehr *et al.*, 2003), which is classically not considered to be functional with regard to N<sub>2</sub> fixation. Organisms associated with cluster IV, which actively fix N<sub>2</sub>, usually contain an additional cluster I or III nitrogenase, which was not detectable in our samples. Thus, we cannot fully exclude that P1 is associated with a non-N<sub>2</sub>-fixing microorganism.

The measured high N<sub>2</sub> fixation rate (800 μmol N m<sup>-2</sup> d<sup>-1</sup>) detected at this sulphidic station indicates that sulphidic events, which have previously been reported to occur in intense OMZs (Naqvi *et al.*, 2000; Lavik *et al.*, 2009) might

sporadically significantly boost N<sub>2</sub> fixation. This might be due to the supply of PO<sub>4</sub><sup>3-</sup> and Fe from the sediment to the water column assuming the sulfidic inputs are sediment derived. Further research in this direction is necessary to establish the potential relationship between these sulfidic events, which develop in nitrogen-depleted waters, and the input of new nitrogen through N<sub>2</sub> fixation.

#### Heterotrophic diazotrophy in the OMZ off Peru

To investigate heterotrophic N<sub>2</sub> fixation in the Peruvian OMZ, we performed glucose and oxygen manipulation experiments at one open ocean station (no.3, 10°S 81.3°W, Figure 1) and one coastal station (no.807, 10.001°S 78.38°W, Figure 1). In both experiments, N<sub>2</sub> fixation was stimulated by the addition of glucose (2 μM) as well as by the simultaneous addition of glucose and oxygen (10 μM) pointing towards a contribution of heterotrophic diazotrophs to N<sub>2</sub> fixation. However, only the glucose effect was significant (Supplementary

Table S2). *nifH* analysis of end points of 24-h  $^{15}\text{N}_2$ -incubation experiments at station 3 (95 m water depth) supplemented with glucose or  $\text{O}_2$  or a combination of both demonstrated the exclusive presence of P4 and P7 *nifH* genes in the different treatments. P1 was present in abundances close to the detection limit in the control and in the glucose treatment (Figure 6; Supplementary Figure S7 shows a similar experiment at the more coastal station 807 from 20-m water depth). For both P4 and P7, there was a conspicuous interaction of glucose with  $\text{O}_2$ : in P4, combined glucose and  $\text{O}_2$  addition resulted in a marked increase of gene abundances compared with a (borderline) significant decrease with only one treatment factor applied (see Supplementary Material and Supplementary Table S2 for details of the statistical analysis). Combined glucose and  $\text{O}_2$  addition resulted in a clear decrease of P7 gene abundances compared with the glucose-only treatment. Gene abundances of cluster P1 did not show any systematic response to the experimental treatment (see Figure 6) and were therefore not further addressed statistically.

Highest  $\text{N}_2$  fixation rates in this experiment were measured in the combined glucose and oxygen addition experiment (*in situ*  $\text{O}_2$  concentrations  $\sim 1.85 \mu\text{M}$ ), which stimulated exclusively the growth of P7, whereas clusters P1 and P4 were negatively affected by the addition of oxygen, even in the presence of glucose. This suggests a potential switch to a dominance of the P7 cluster when  $\text{O}_2$  is transported into the OMZ (for example, by  $\text{O}_2$  intrusions or vertical mixing), thus demonstrating the capability of the diazotrophic community to react rapidly to changing  $\text{O}_2$  conditions. The increase in  $\text{N}_2$  fixation with the addition of glucose in both experiments (no.3, 95 m; and no.807, 20 m) points towards a heterotrophic mode of diazotrophy

throughout the OMZ that might be limited by the availability of reduced carbon compounds rather than by nutrients.

#### Co-occurrence of $\text{N}_2$ fixation and N-loss processes

Evidence for the co-occurrence of N-loss and  $\text{N}_2$  fixation mainly ascribed to *Chlorobium*-like diazotrophs has previously been documented for an anoxic lake (Halm *et al.*, 2009) and is proposed to have a major role in marine  $\text{N}_2$  fixation as well (Deutsch *et al.*, 2007). As mentioned above, Deutsch *et al.* (2007) predicted that the availability of excess phosphorous resulting from N-loss processes in the OMZ off Peru is favourable for  $\text{N}_2$  fixation. The dominance of heterotrophic diazotrophs along with active  $\text{N}_2$  fixation in waters below the oxycline implies the possibility for a close spatial coupling of N-loss and  $\text{N}_2$  fixation. Kalvelage *et al.* (2013) reported in their N-loss study from the same cruise that denitrification rates in the water column were not detectable except for two shelf stations (note that one of those was no.807 at 20 m with a denitrification rate of  $5.42 \text{ nmol l}^{-1} \text{ d}^{-1}$ , which has been discussed above with regard to  $\text{N}_2$  fixation rates) and the sulphidic station. In the presence of  $\text{H}_2\text{S}$ , water column denitrification ranged from  $126 \text{ nmol N l}^{-1} \text{ d}^{-1}$  to  $2068 \text{ nmol N l}^{-1} \text{ d}^{-1}$ , indicating a coupling with  $\text{N}_2$  fixation rates, which are significantly positively correlated to denitrification rates ( $n=5$ ,  $r^2=0.59$ ) at that station. *nifH* gene abundances of cluster P1 coincided with the denitrification key functional gene *nirS* (coding for the cd1-containing nitrite reductase) on the shelf at  $10^\circ\text{S}$  (Supplementary Figures S2 and S8). Overall, Kalvelage *et al.* (2013) reported that anammox was the major N-loss process during the sampling period in that area and was detectable at all stations from the coast to  $84^\circ\text{W}$ , with highest rates ( $\leq 225 \text{ nmol N l}^{-1} \text{ d}^{-1}$ ) over the central

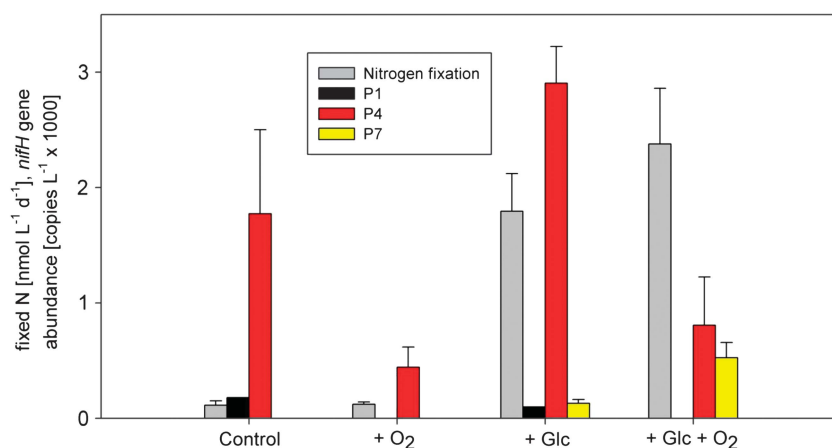


**Figure 6** The effect on the addition of glucose ( $2 \mu\text{M}$ ) and oxygen ( $10 \mu\text{M}$ ) on  $\text{N}_2$  fixation as well as on the *nifH* gene abundances of the detectable clusters P1, P4 and P7 (both as end point measurements in 24-h incubations, samples from no.3, 95 m) were determined. S.d.s. of triplicate measurements are indicated, with the exception of P1 which was below the detection limit in two of three replicate samples. Rates are a minimum value of  $\text{N}_2$  fixation due to a probable underestimation by the applied method.

shelf (10°S–16°S) declining by two orders of magnitude towards the open ocean. Similarly, N<sub>2</sub> fixation rates were higher on the shelf, declining by one to two orders of magnitude towards the open ocean (compare Figure 5, Supplementary Figures S5 and S6). This co-occurrence of N<sub>2</sub> fixation and anammox is in line with the significant correlation of gene abundances of P1 and the hydrazine (N<sub>2</sub>H<sub>4</sub>) oxidoreductase anammox key gene *hzo* ( $n = 113$ ,  $r^2 = 0.591$ ) and a correlation of total *nifH* and *hzo* ( $n = 113$ ,  $r^2 = 0.544$ ), both observed at 10°S. Both *nifH* gene abundance (see above) and anammox rates (Kalvelage *et al.*, 2013) were significantly correlated to NO<sub>2</sub><sup>-</sup> concentrations on the shelf. Further, *nifH* gene abundances of cluster P1 correlated significantly with the abundances of key functional genes of archaeal ammonia oxidation (archaeal *amoA*, coding for the ammonia monooxygenase,  $n = 351$ ,  $r = 0.61$ ) on the shelf pointing towards a close spatial coupling of all detected N turnover processes in this area.

Based on our findings, we hypothesize, that a close coupling of N-loss processes and N<sub>2</sub> fixation exists in OMZs and that N<sub>2</sub> fixation may be responsible for the progressive increase in N:P ratio from the inshore waters to the open ocean as previously suggested by the model study of Deutsch *et al.* (2007).

## Conclusions

Our study demonstrates the presence of mainly heterotrophic diazotrophs in the OMZ off Peru. High primary production close to the coast might fuel heterotrophic diazotrophy in this area supported by the presence of elevated iron across the shelf region. In light of our results, this heterotrophic N<sub>2</sub> fixation seems to be directly linked to anammox and other N-turnover processes, thus in principle confirming the model of Deutsch *et al.* (2007). However, in contrast to the suggestion of Deutsch *et al.* (2007) that the highest N<sub>2</sub> fixation occurs in oligotrophic open ocean waters towards the South Pacific Gyre, our results support a much closer spatial coupling of N loss and N<sub>2</sub> fixation, with the highest rates in shelf waters with high organic matter load and high iron availability. Contrary to the classical view, the diazotrophic distribution can statistically be explained by factors other than O<sub>2</sub> and NO<sub>3</sub><sup>-</sup>, namely NO<sub>2</sub><sup>-</sup> and PO<sub>4</sub><sup>3-</sup>. The activity of diazotrophs in waters below the euphotic zone has currently not been considered in estimates of global N<sub>2</sub> fixation rates neither from biogeochemical models (Codispoti, 2007) nor derived from geochemical tracer studies or direct measurements. Our findings may therefore facilitate a more realistic estimation of the marine nitrogen budget with regard to ocean de-oxygenation.

Furthermore, our findings contribute to the emerging view that the habitat of diazotrophs should be extended towards high fixed nitrogen environments in OMZs in which a unique diazotrophic community exists.

## Conflict of Interest

The authors declare no conflict of interest.

## Acknowledgements

We thank the authorities of Peru for granting permission to work in their territorial waters. We acknowledge the support of the captain and crew of the R/V *Meteor* as well as the chief scientists Martin Frank and Lothar Stramma. Moreover, we thank I Grefe for sampling during M77/4 and O Baars and A Dammshäuser for trace metal sampling during M77/3; we also thank G Klockgether, K Stange, F Malien, V Leon and P Fritsche for oxygen and nutrient measurements, and also G Klockgether and P Streu for assisting with the mass spectrometry and trace metal analyses, respectively. We thank Hermann Bange, V Bertics and K Wuttig for helpful discussion. Financial support for this study was provided by the DFG Sonderforschungsbereich 754 ([www.sfb754.de](http://www.sfb754.de)) and the Max Planck Society (MPG).

## Author contributions

CRL, TG, HS and JLR collected samples and performed the experiments onboard. CRL and DG and FDD extracted the DNA. CRL and DG performed the qPCR of *nifH* genes from transect stations. FDD designed primers and probes for *nifH* qPCRs. CRL, TG, NP, FDD and DG cloned *nifH* gene fragments. TG, CRL and HS extracted DNA and RNA from experimental stations. TG and CRL performed *nifH* qPCRs of experimental stations. CRL performed *amoA*, *hzo* and *nirS* qPCRs of M77/3 stations. TG performed flow cytometry measurements and analysed the C and N fixation data. SCN performed the statistical analysis. CS and PLC performed the trace metal sampling and analysis. CRL wrote the manuscript with TG, HS, RAS and JLR. MMMK, GL, RAS, JLR, TG and CRL designed the experiments and analysed the data.

## References

- Bopp L, Le Quere C, Heimann M, Manning AC, Monfray P. (2002). Climate-induced oceanic oxygen fluxes: implications for the contemporary carbon budget. *Global Biogeochem Cycles* **16**: 14.
- Bruland KW, Franks RP, Knauer GA, Martin JH. (1979). Sampling and analytical methods for the determination of copper, cadmium, zinc, and nickel at the nanogram per liter level in sea water. *Anal Chim Acta* **105**: 233–245.
- Bruland KW, Rue EL, Smith GJ, DiTullio GR. (2005). Iron, macronutrients and diatom blooms in the Peru upwelling regime: brown and blue waters of Peru. *Mar Chem* **93**: 81–103.
- Capone D. (2008). The marine nitrogen cycle. *Microbe* **3**: 186–192.
- Capone DG, Burns JA, Montoya JP, Subramaniam A, Mahaffey C, Gunderson T *et al.* (2005). Nitrogen



- fixation by *Trichodesmium* spp.: an important source of new nitrogen to the tropical and subtropical North Atlantic Ocean. *Global Biogeochem Cycles* **19**: 17.
- Church MJ, Jenkins BD, Karl DM, Zehr JP. (2005). Vertical distributions of nitrogen-fixing phylotypes at Stn ALOHA in the oligotrophic North Pacific Ocean. *Aquat Microb Ecol* **38**: 3–14.
- Codispoti LA. (2007). An oceanic fixed nitrogen sink exceeding 400 Tg Na(-1) vs the concept of homeostasis in the fixed-nitrogen inventory. *Biogeosciences* **4**: 233–253.
- Codispoti LA. (2010). Interesting times for marine N<sub>2</sub>O. *Science* **327**: 1339–1340.
- Danielsson L-G, Magnusson B, Westerlund S. (1978). An improved metal extraction procedure for the determination of trace metals in sea water by atomic absorption spectrometry with electrothermal atomization. *Anal Chim Acta* **98**: 47–57.
- Deutsch C, Gruber N, Key RM, Sarmiento JL, Ganachaud A. (2001). Denitrification and N<sub>2</sub> fixation in the Pacific Ocean. *Global Biogeochem Cycles* **15**: 483–506.
- Deutsch C, Sarmiento JL, Sigman DM, Gruber N, Dunne JP. (2007). Spatial coupling of nitrogen inputs and losses in the ocean. *Nature* **445**: 163–167.
- Duce RA, LaRoche J, Altieri K, Arrigo KR, Baker AR, Capone DG *et al.* (2008). Impacts of atmospheric anthropogenic nitrogen on the open ocean. *Science* **320**: 893–897.
- Falcon LI, Cipriano F, Chistoserdov AY, Carpenter EJ. (2002). Diversity of diazotrophic unicellular cyanobacteria in the tropical North Atlantic Ocean. *Appl Environ Microbiol* **68**: 5760–5764.
- Farnelid H, Bentzon-Tilia M, Andersson AF, Bertilsson S, Jost G, Labrenz M *et al.* (2013). Active nitrogen-fixing heterotrophic bacteria at and below the chemocline of the central Baltic Sea. *ISME J* **7**: 1413–1423.
- Farnelid H, Andersson AF, Bertilsson S, Al-Soud WA, Hansen LH, Sørensen S *et al.* (2011). Nitrogenase gene amplicons from global marine surface waters are dominated by genes of non-cyanobacteria. *PLoS One* **6**: e19223.
- Fernandez C, Farias L, Ulloa O. (2011). Nitrogen fixation in denitrified marine waters. *PLoS One* **6**: 9.
- Franz J, Krahnemann G, Lavik G, Grasse P, Dittmar T, Riebesell U. (2012). Dynamics and stoichiometry of nutrients and phytoplankton in waters influenced by the oxygen minimum zone in the eastern tropical Pacific. *Deep-Sea Res Pt I* **62**: 20–31.
- Gandhi N, Singh A, Prakash S, Ramesh R, Raman M, Sheshshayee MS *et al.* (2011). First direct measurements of N<sub>2</sub> fixation during a *Trichodesmium* bloom in the eastern Arabian Sea. *Global Biogeochem Cycles* **25**: 10.
- Grasshoff G, Kremling K, Erhardt M. (1999). *Methods of Seawater Analysis*. Wiley VCH: Weinheim, Germany.
- Grosskopf T, LaRoche J. (2012). Direct and indirect costs of dinitrogen fixation in *Crocospaera watsonii* WH8501 and possible implications for the nitrogen cycle. *Front Aquat Microbiol* **3**: 236.
- Grosskopf T, Mohr W, Baustian T, Schunck H, Gill D, Kuypers MMM *et al.* (2012). Doubling of marine dinitrogen-fixation rates based on direct measurements. *Nature* **488**: 361–364.
- Halm H, Lam P, Ferdelman TG, Lavik G, Dittmar T, LaRoche J *et al.* (2012). Heterotrophic organisms dominate nitrogen fixation in the South Pacific Gyre. *ISME J* **6**: 1238–1249.
- Halm H, Musat N, Lam P, Langlois R, Musat F, Peduzzi S *et al.* (2009). Co-occurrence of denitrification and nitrogen fixation in a meromictic lake, Lake Cadagno (Switzerland). *Environ Microbiol* **11**: 1945–1958.
- Hamersley MR, Turk KA, Leinweber A, Gruber N, Zehr JP, Gunderson T *et al.* (2011). Nitrogen fixation within the water column associated with two hypoxic basins in the Southern California Bight. *Aquat Microb Ecol* **63**: 193.
- Hong H, Kester DR. (1986). Redox state of iron in offshore waters of Peru. *Limnol Oceanogr* **31**: 512–524.
- Hutchins DA, Hare CE, Weaver RS, Zhang Y, Firme GF, DiTullio GR *et al.* (2002). Phytoplankton iron limitation in the Humboldt Current and Peru Upwelling. *Limnol Oceanogr* **47**: 997–1011.
- Ingall E, Jahnke R. (1994). Evidence for enhanced phosphorus regeneration from marine sediments overlain by oxygen depleted waters. *Geochim Cosmochim Acta* **58**: 2571–2575.
- Jayakumar A, Al-Rshaidat MMD, Ward BB, Mulholland MR. (2012). Diversity, distribution, and expression of diazotroph nifH genes in oxygen-deficient waters of the Arabian Sea. *FEMS Microbiol Ecol* **82**: 597–606.
- Kalvelage T, Lavik G, Lam P, Contreras S, Artega L, Löscher CR *et al.* (2013). Nitrogen cycling driven by organic matter export in the South Pacific oxygen minimum zone. *Nat Geosci* **6**: 228–234.
- Lam P, Jensen MM, Lavik G, McGinnis DF, Muller B, Schubert CJ *et al.* (2007). Linking crenarchaeal and bacterial nitrification to anammox in the Black Sea. *Proc Natl Acad Sci USA* **104**: 7104–7109.
- Lane BG, Bernier F, Dratewka-Kos E, Shafai R, Kennedy TD, Pyne C *et al.* (1991). Homologies between members of the germin gene family in hexaploid wheat and similarities between these wheat germins and certain Physarum spherulins. *J Biol Chem* **266**: 10461–10469.
- Langlois RJ, LaRoche J, Raab PA. (2005). Diazotrophic diversity and distribution in the tropical and subtropical Atlantic ocean. *Appl Environ Microbiol* **71**: 7910–7919.
- Langlois RJ, Hummer D, LaRoche J. (2008). Abundances and distributions of the dominant nifH phylotypes in the Northern Atlantic Ocean. *Appl Environ Microbiol* **74**: 1922–1931.
- Lavik G, Stuhmann T, Bruchert V, Van der Plas A, Mohrholz V, Lam P *et al.* (2009). Detoxification of sulphidic African shelf waters by blooming chemolithotrophs. *Nature* **457**: 581–U586.
- Legendre P, Gallagher ED. (2001). Ecologically meaningful transformations for ordination of species data. *Oecologia* **129**: 271–280.
- Loescher CR, Kock A, Koenneke M, LaRoche J, Bange HW, Schmitz RA. (2012). Production of oceanic nitrous oxide by ammonia-oxidizing archaea. *Biogeosci Discuss* **9**: 2095–2122.
- Mohr W, Grosskopf T, Wallace DWR, LaRoche J. (2010). Methodological underestimation of oceanic nitrogen fixation rates. *PLoS One* **5**: e12583.
- Montoya JP, Voss M, Kahler P, Capone DG. (1996). A simple, high-precision, high-sensitivity tracer assay for N<sub>2</sub> fixation. *Appl Environ Microbiol* **62**: 986–993.
- Naqvi SWA, Jayakumar DA, Narveka PV, Naik H, Sarma VVSS, D'Souza W *et al.* (2000). Increased marine production of N<sub>2</sub>O due to intensifying anoxia on the Indian continental shelf. *Nature* **408**: 346–349.

- Oksanen J, Blanchet FG, Kindt R, Legendre P, Minchin PR, O'Hara RB *et al.* (2013). *vegan*: Community ecology package. R package version 2.0-10. <http://CRAN.R-project.org/package=vegan>.
- R\_Core\_Team. (2013). R: A language and environment for statistical computing. In: <http://www.R-project.org/>.
- Schmid MC, Hooper AB, Klotz MG, Woebken D, Lam P, Kuypers MMM *et al.* (2008). Environmental detection of octahaem cytochrome c hydroxylamine/hydrazine oxidoreductase genes of aerobic and anaerobic ammonium-oxidizing bacteria. *Environ Microbiol* **10**: 3140–3149.
- Schunck H, Lavik G, Desai DK, Großkopf T, Kalvelage T, Löscher CR *et al.* (2013). Giant hydrogen sulfide plume in the oxygen minimum zone off Peru supports chemolithoautotrophy. *PLoS One* **8**: e68661.
- Stratil SB, Neulinger SC, Knecht H, Friedrichs AK, Wahl M. (2013). Temperature-driven shifts in the epibiotic bacterial community composition of the brown macroalga *Fucus vesiculosus*. *Microbiologyopen* **2**: 338–349.
- Turk KA, Rees AP, Zehr JP, Pereira N, Swift P, Shelley R *et al.* (2011). Nitrogen fixation and nitrogenase (*nifH*) expression in tropical waters of the eastern North Atlantic. *ISME J* **5**: 1201–1212.
- Ullrich W, Rigano C, Fuggi A, Aparicio P, Paneque A, Cejudo FJ *et al.* (1990). Nitrogen metabolism in heterotrophic bacteria. Simultaneous ammonia inhibition of nitrogen fixation and nitrate uptake and divalent anion regulation of nitrate uptake in *Azotobacter chroococcum*. In *Inorganic Nitrogen in Plants and Microorganisms*. Springer: Berlin, Heidelberg, Germany, pp 93–98.
- Zani S, Mellon MT, Collier JL, Zehr JP. (2000). Expression of *nifH* genes in natural microbial assemblages in Lake George, New York, detected by reverse transcriptase PCR. *Appl Environ Microbiol* **66**: 3119–3124.
- Zehr JP, Turner PJ. (2001). Nitrogen fixation: nitrogenase genes and gene expression. In: *Methods in Microbiology* vol 30. Academic Press Inc: San Diego, CA, USA, pp 271–286.
- Zehr JP, Mellon MT, Zani S. (1998). New nitrogen-fixing microorganisms detected in oligotrophic oceans by amplification of nitrogenase (*nifH*) genes (vol 64, pg 3444, 1998). *Appl Environ Microbiol* **64**: 5067.
- Zehr JP, Jenkins BD, Short SM, Steward GF. (2003). Nitrogenase gene diversity and microbial community structure: a cross-system comparison. *Environ Microbiol* **5**: 539–554.

Supplementary Information accompanies this paper on The ISME Journal website (<http://www.nature.com/ismej>)